GEOPHYSICS, VOL. 69, NO. 2 (MARCH-APRIL 2004); P. 318–329, 13 FIGS.
10.1190/1.1707051

Case History

Downhole seismic imaging of a massive sulfide orebody with mode-converted waves, Halfmile Lake, New Brunswick, Canada

Gilles Bellefleur*, Christof Müller‡, David Snyder*, and Larry Matthews**

ABSTRACT

Multioffset, multiazimuth downhole seismic data were acquired at Halfmile Lake, New Brunswick, to image known massive sulfide lenses and to investigate the potential existence of a steeply dipping mineralized zone connecting them. The massive sulfide lenses, which have significantly higher elastic impedances than host rocks, produce strong scattering. The downhole seismic data show prominent scattered (P-P and S-S) and mode-converted (P-S and S-P) waves originating from the deposit. Such complex scattering from massive sulfide ore was not observed previously in vertical seismic profiling data. Migration of the scattered and mode-converted waves from several shot points imaged different parts of the deepest lens. The scattered S-waves and mode-converted waves provide additional imaging capabilities that should be considered when selecting downhole seismic methods for mining exploration.

INTRODUCTION

The eastern Canadian mining industry faces a decrease in known base metal reserves in mature mining camps and strives to find new resources to sustain the existing ore processing infrastructure. The search for new resources often involves deeper exploration programs that require new tools and techniques to detect deposits and to efficiently direct deep and costly boreholes. With encouraging results recently obtained at various mining camps, seismic methods are becoming increasingly relevant to the deep exploration for massive sulfide deposits (Adam et al., 2000; Milkereit et al., 2000; Salisbury et al., 2000; Eaton, Milkereit, et al., 2003). Seismic exploration for massive sulfide deposits has largely utilized P-wave energy reflected or scattered at mineralized zones. However, elastic-wave theory and finite-difference modeling predict that base metal deposits can convert a significant part of the incident seismic energy, producing converted waves potentially useful for mining exploration (Bohlen et al., 2003). In practice, converted waves are not considered in mining exploration because they are rarely recognized or observed in the seismic data. Here, we present prominent scattered (P-P and S-S) and mode-converted (P-S and S-P) waves originating from a deep massive sulfide lens at Halfmile Lake, New Brunswick, Canada.

The scattered and mode-converted waves were observed on multioffset and multiazimuth vertical seismic profiling (VSP) data acquired by the Downhole Seismic Imaging (DSI) consortium. This consortium was initiated by the Geological Survey of Canada, Canadian mining and services companies (Falconbridge, Inco, Quantec Geoscience, and Noranda), and universities (University of Western Ontario, University of Alberta, Memorial University, Christian Albrechts University in Kiel, Cambridge University, and the University of Helsinki) to further demonstrate the utility of VSP for exploration of massive sulfide deposits in areas with steeply dipping stratigraphy. The VSP geometry has been shown to be more appropriate than surface seismic surveying for mineral exploration in regions characterized by steep geological dips (Eaton, Guest, et al., 1996; Adam et al., 2003). The Halfmile Lake deposit is an appealing target because it contains massive sulfide lenses of known geometry embedded in a steeply dipping stratigraphy, and the ore contrasts significantly in impedance with the almost seismically transparent host rocks (Salisbury et al., 2000). After reviewing the geological setting, the physical rock properties, and previous seismic work, we present results

Manuscript received by the Editor January 24, 2002; revised manuscript received October 15, 2003.
*Geological Survey of Canada, 615 Booth Street, Room 207, Ottawa, Ontario K1A 0E9, Canada. E-mail: gbellefl@nrcan.gc.ca.
‡Formerly Geological Survey of Canada, Ottawa, Ontario, K1A 0E9, Canada; presently Christian Albrechts University, Otto-Hahn-Platz 1, D-24118, Kiel, Germany.
**Formerly Mira Geoscience, Calgary, Alberta, Canada; presently Hampson Russell, Suite 510, 715-5th Avenue SW, Calgary, Alberta T2P 2X6, Canada.

indicating that scattered S-waves and mode-converted waves should be considered when planning a seismic survey, as well as in processing and imaging seismic data to detect massive sulfide deposits.

GEOLOGICAL SETTING

The Halfmile Lake deposit is located in the Bathurst mining district in New Brunswick, Canada (Figure 1). The shallow part of the deposit was discovered by Middle River Mining Co. (Texas Gulf Sulphur Co.) in 1955 as a result of follow-up work on coincident EM airborne and soil geochemical anomalies (Thomas et al., 2000). The deposit is part of the Middle Ordovician Tetagouche Group, a bimodal volcanic and sedimentary sequence hosting several zinc/lead/copper deposits within a subcircular area 50 km in diameter (McCutcheon, 1992). The Halfmile Lake volcanogenic massive sulfide deposit, with 25 million tons of total sulfide content, is the largest undeveloped deposit within the mining district. Mineralization consists of pyrrhotite-rich breccia-matrix sulfides and pyrite–pyrrhotite-rich layered sulfides distributed in a laterally continuous sheet (Adair, 1992). The deposit is hosted by a sequence of felsic volcanic rocks, interbedded sedimentary epiclastic rocks, intrusive subvolcanic porphyries, and mafic volcanic rocks. Folding of the stratigraphic sequence placed the deposit on the south limb of an overturned antiform (Figure 2), where the average dip is 45° to the north–northwest. However, the sulfide sheet is irregular and steepens locally from multiple periods of fold deformation. Significant concentrations of sulfides occur in three zones (upper, lower, and deep zones, Figure 2) where thicknesses reach 50 m. The lower and deep zones and an area of steeply dipping stratigraphy connecting them are investigated in this study.

PHYSICAL ROCK PROPERTIES AND PREVIOUS SEISMIC WORK

The first seismic surveys at Halfmile Lake were combined with physical rock property measurements to assess the P-wave

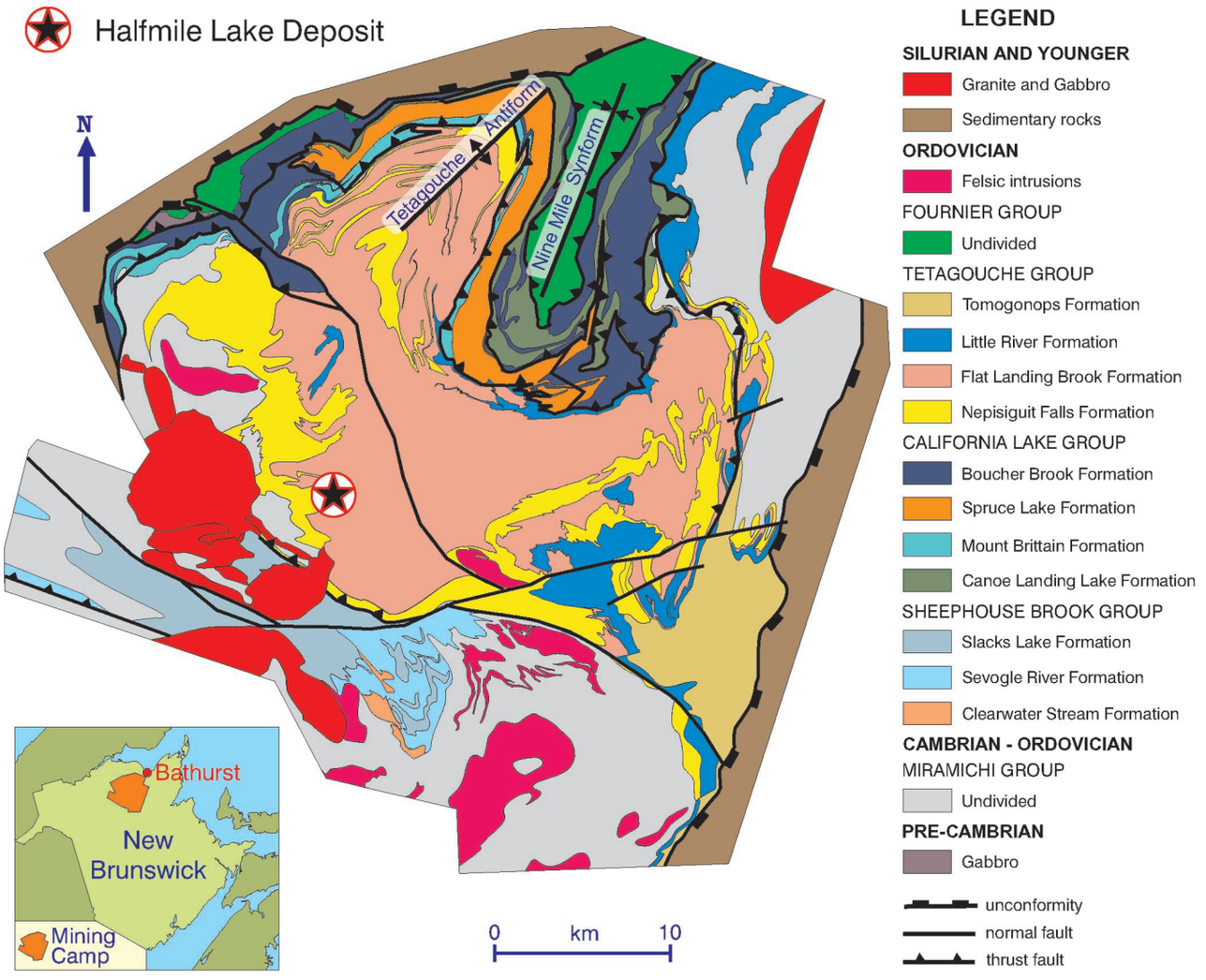

Figure 1. Geology map of Bathurst Mining camp, modified from Thomas et al. (2000). The Halfmile Lake deposit is located in the southwestern part of the camp (star).

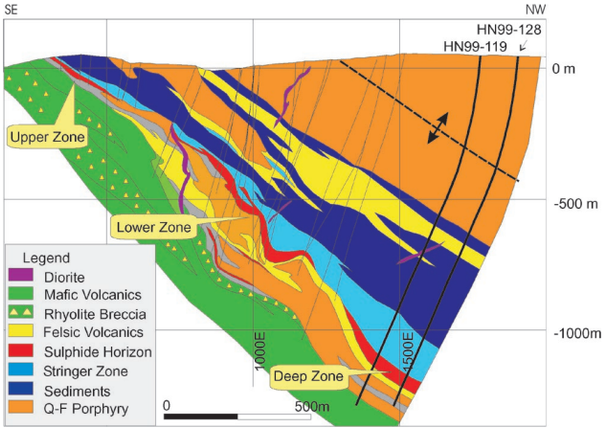

Figure 2. Composite geologic cross-section through Halfmile Lake deposit based on projection of drilling results to a southeast–northwest section (looking southwest). Borehole HN99-128 was used for the VSP survey. Density and sonic logs were collected in borehole HN99-119. The lower and deep lenses and the area of steeply dipping stratigraphy between them were the targets of the survey. See Figure 5 for surface location of the cross-section.

reflectivity of the massive sulfides and the surrounding geological units. Acoustic impedance measurements on ore samples from the upper and lower lenses and the host rocks indicated that the sulfides should be strong P-wave reflectors (Salisbury et al., 2000). Similar conclusions were obtained from velocity and density logs measured in two boreholes intersecting the lower and deep lenses [see Salisbury et al. (2000) for logs in a borehole intersecting the lower lens and Figure 3 for the deep lens borehole logs]. Furthermore, synthetic traces calculated by convolving the reflection coefficients determined from one of the borehole logs with a 50-Hz Ricker wavelet also show that host rocks are generally weakly reflective or seismically transparent, whereas the ore should produce a strong P-wave reflection (Figure 3).

Full-waveform sonic logging in borehole HN99-119 determined the S-wave velocity of the host rocks and massive sulfides (Figure 4). Synthetic seismic traces, calculated by convolving the measured S-wave reflection coefficients with a 50-Hz Ricker wavelet, predict that the deep massive sulfide lens is a strong S-wave reflector. All borehole logs demonstrate that the deep lens and host rocks have contrasting physical rock properties sufficient to generate significant converted waves.

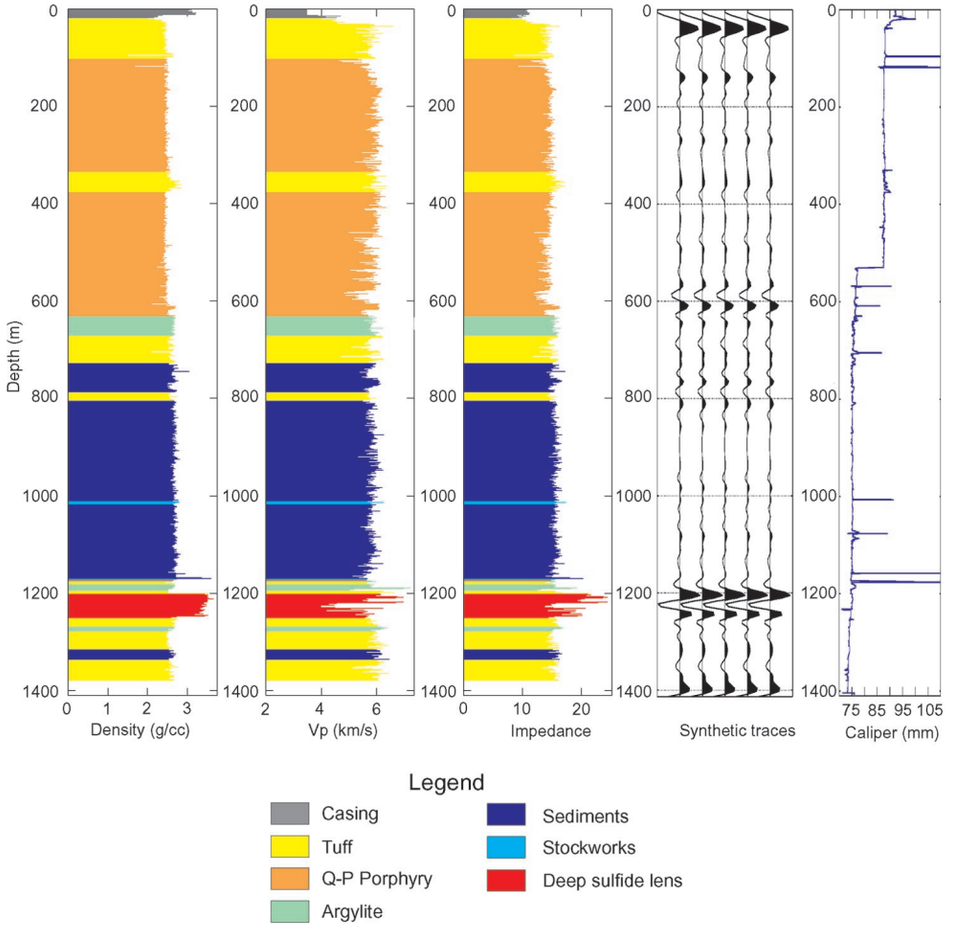

Figure 3. Density, P-wave velocity, impedance, synthetic traces, and caliper log for borehole HN-99-119. The synthetic traces were calculated by convolving the reflectivity series with a 50-Hz Ricker wavelet. A prominent reflection is expected from the deep sulfide lens at 1200 m. A weaker reflection at 600 m does not correspond directly with a lithological change. Caliper log shows irregular borehole walls. The acquisition borehole (HN99-128) intersects the same rock units and presumably has similar rugose walls. The top part of the hole was drilled with an HQ bit (95 mm); whereas, the lower part was drilled with an NQ bit (76 mm). HQ and NQ drill bits were also used for the acquisition borehole. See Figure 5 for location of the borehole.

A near-offset VSP (source–borehole offset of 100 m) acquired in 1994 in a borehole intersecting the lower zone showed prominent reflections from sulfides at depth (Salisbury et al., 2000). In 1995 and 1996, Noranda acquired two surface-recorded seismic 2D profiles. The 1995 profile imaged a high-amplitude anomaly corresponding to the lower zone and was the first direct indication that massive sulfides could be detected with surface seismic methods in this area. Additional amplitude anomalies were also identified on the 1996 2D profile. A follow-up 3D seismic survey in 1998 determined the position and geometry of these anomalies and led to the discovery of the deep zone, which contains an estimated 15.7 million tons of sulfides (Matthews, 2002). Surface seismic data could have improved processing and interpretation of the VSP data presented here but were not used to demonstrate the potential of the downhole seismic method for mineral exploration.

DATA ACQUISITION AND PROCESSING

The acquisition geometry used at Halfmile Lake (Figure 5) was based on traveltime modeling using known positions of the lower and deep sulfide lenses and the assumed area of subvertical stratigraphy connecting them. The modeling approach followed the procedure described in Adam et al. (2003). The shot locations were optimized to provide maximum scattered P-wave energy from the deposit for given receiver positions in the borehole. The survey was comprised of two parts. Initially, four source locations were selected (sites A, B, C, and D on Figure 5) at which a total of 104 shots were fired (26 at each site). Receiver depths ranged between 265 and 1300 m with a 5-m interval. Shots were then placed along a shot line used during an earlier surface 3D seismic survey. At each station along

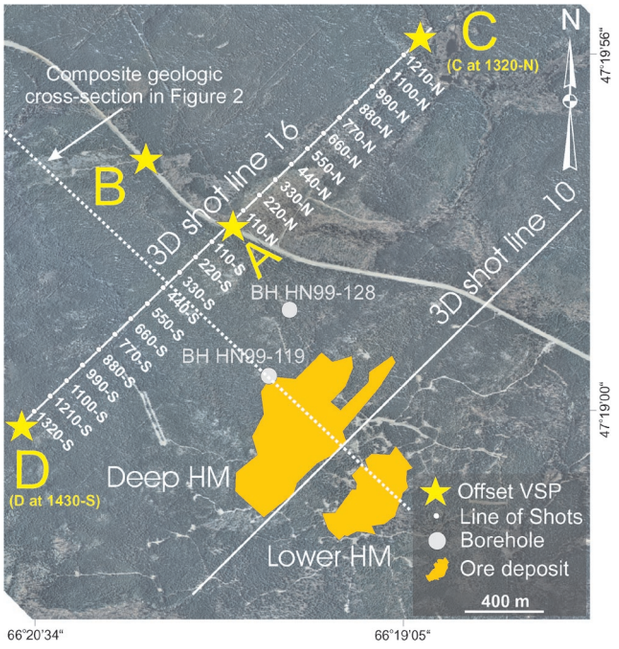

Figure 5. Acquisition geometry used at Halfmile Lake. The survey was divided into two parts. The first part consisted of four offset VSPs. The shots for this part of the survey are indicated by yellow stars. Recording depths in borehole HN99-128 ranged between 265 and 1300 m. For the second part of the survey, shots were distributed along a line between stations 1320S and 1210N. Three shots were fired at each station for this walkaway geometry. Recording depths ranged from 585 to 815 m.

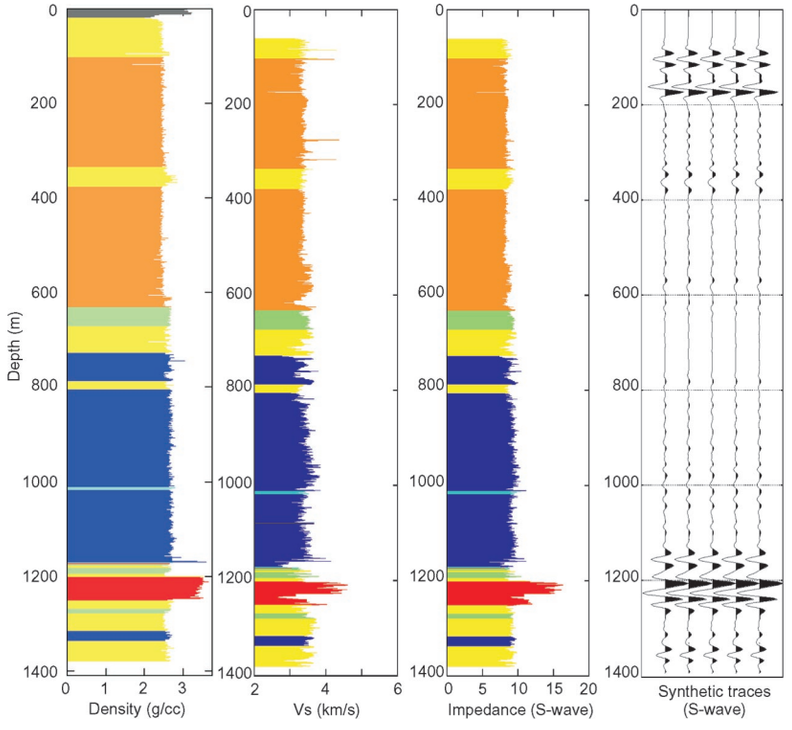

Figure 4. Density, S-wave velocity, impedance, and synthetic traces calculated by convolving the reflectivity series with a 50-Hz Ricker wavelet. A strong S-wave reflection is expected from the deep sulfide lens. See Figure 3 for geological legend.

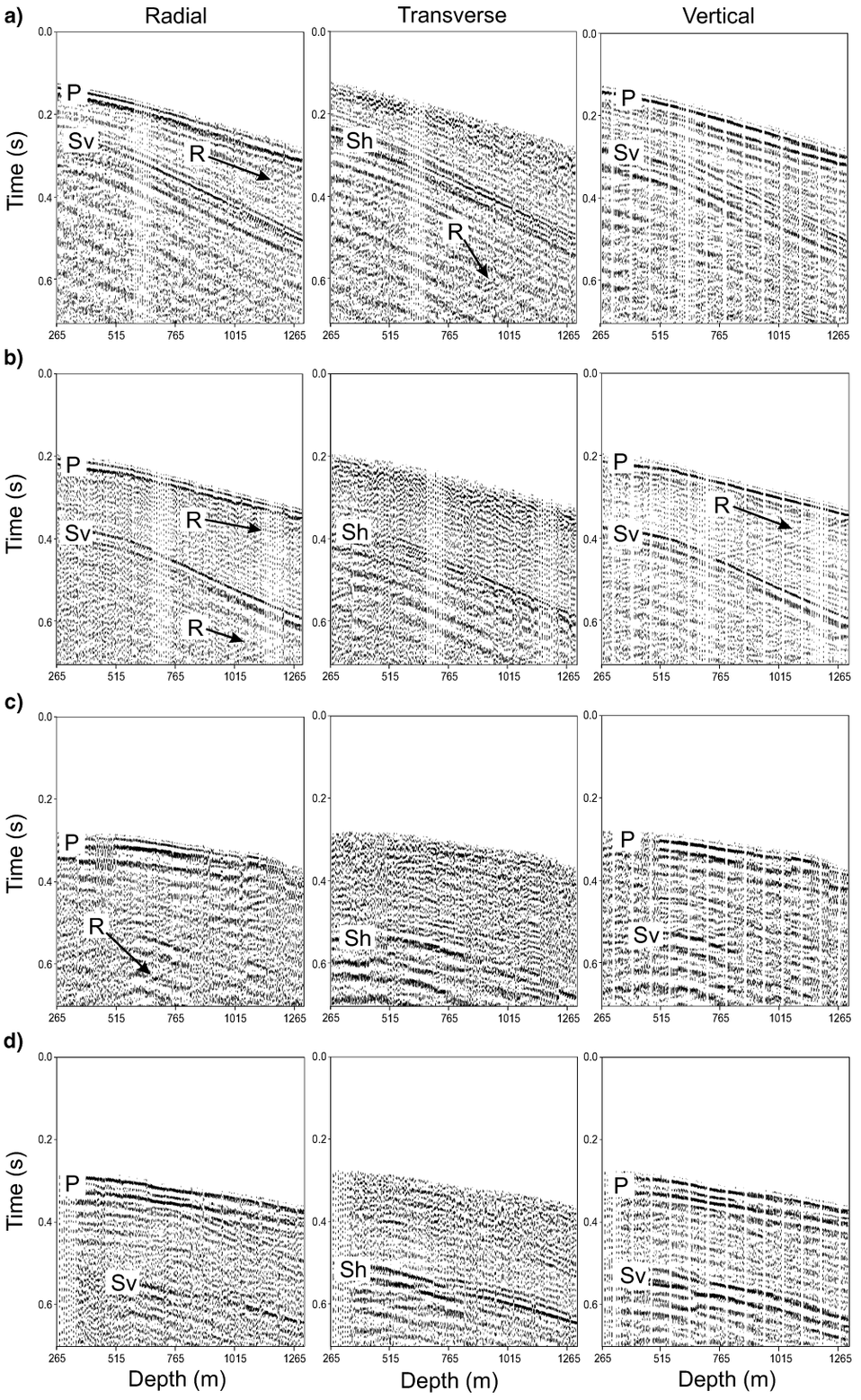

Figure 6. Direct arrivals observed on the radial, transverse, and vertical components from shot sites (a) A, (b) B, (c) C, and (d) D. Various events are annotated: P (direct P-wave); S_v and S_h (direct S-wave); R (reflection). The S_v-waves are polarized in the vertical plane defined by the source location and borehole; polarizations of S_h-waves are orthogonal to that plane. An automatic gain control (AGC) (0.2-s window) has been applied.

this line (white dots marked 1320S to 1210N on Figure 5), three shots were fired for receiver depths between 585 and 815 m with a 10-m interval. This walkaway geometry was selected to image the lateral extent of the sulfide sheet at specific depths, whereas the full-offset VSPs would image the vertical extent of the dipping sulfide sheet at specific locations.

The recording borehole (HN99-128) was the only hole out of 12 boreholes that remained open in this area of the Halfmile camp. All boreholes were cased over the unconsolidated overburden (approximately 5 m), and most deformed and became blocked since their drilling in 1999. At the surface, borehole HN99-128 is located approximately 600 m north of the deep lens. It deviates from the vertical by 10° at shallow depths and by 18° at 1336.5 m where it intersects the deep lens. The top and bottom parts of the borehole were drilled with HQ (hole diameter of 95 mm) and NQ (hole diameter of 76 mm) bits, respectively. The slim downhole receiver unit comprised eight levels with three orthogonal 28-Hz geophones. The source consisted of three 227-g pentolite boosters placed in 8-m-deep shot holes, which were filled with drilling dust up to the surface. The sampling interval was 0.5 ms with a total record length of 2.1 s. During acquisition, receivers were kept at a specific recording depth to provide constant geophone orientation until traces from all shotpoints were acquired at that depth. Further details about the acquisition geometry, equipment, and parameters can be found in Bellefleur et al. (2002).

Field records are dominated by strong downgoing P- and S-waves (see Figure 6 for offset VSPs and Figure 10 for the walkaway VSP). The upgoing wavefield is relatively weak and is characterized by a few events scattered from the deep sulfide lens near the bottom of the borehole (Figure 6). Processing was critical to reveal waves scattered from the orebody. Particularly important processing steps included band-pass filtering (25–105 Hz) and predictive deconvolution designed to remove a long oscillating coda that followed direct P- and S-wave arrivals on the horizontal components (Figures 7a and 7b). The oscillation is possibly related to mechanical coupling problems with an irregular borehole wall (see caliper log for borehole HN99-119 on Figure 3). Predictive deconvolution was not applied to individual horizontal components but to a combined component with maximized reverberation content (Figure 7c). While attempting to rotate horizontal components into radial and transverse orientations, we observed that reverberations behaved similarly to polarized waves and could be maximized into one component on which the predictive deconvolution provided improved results (Figure 7e). A polarization analysis technique used to orient a triaxial VSP geophone (DiSiena et al., 1984) maximized reverberations on one component. The polarization analysis window consisted of the entire trace without any gain. After deconvolution, the horizontal traces were rotated back to their initial orientation. Particle polarizations of direct P-wave arrivals from all shot locations were statistically analyzed to determine the downhole orientation of the three-component receiver array (Bellefleur et al., 2001) and were used to rotate the horizontal traces into radial and transverse orientations. The inclination of the borehole was taken into account during this transformation. The downgoing P- and S-waves were suppressed using an 11-trace median filter (Hardage, 2000); remaining downgoing waves were removed with f-k filters. A spatial signal detection filter (Kong et al., 1985) based on a semblance-weighted local slant stack was applied to display the processed VSP sections shown in Figures 8 and 9. Some processed records from the walkaway VSP without spatial signal detector filtering are shown in Figure 10.

OREBODY SCATTERING RESPONSE

The Halfmile Lake sulfide lenses are characterized by different shapes and sizes which specifically influenced the scattered seismic wavefield. All lenses can be considered as large inclusions (Eaton, 1999; Bohlen et al., 2003) and should backscatter detectable energy into the upgoing wavefield. In the following subsections, we examine the orebody scattering response for the two survey geometries.

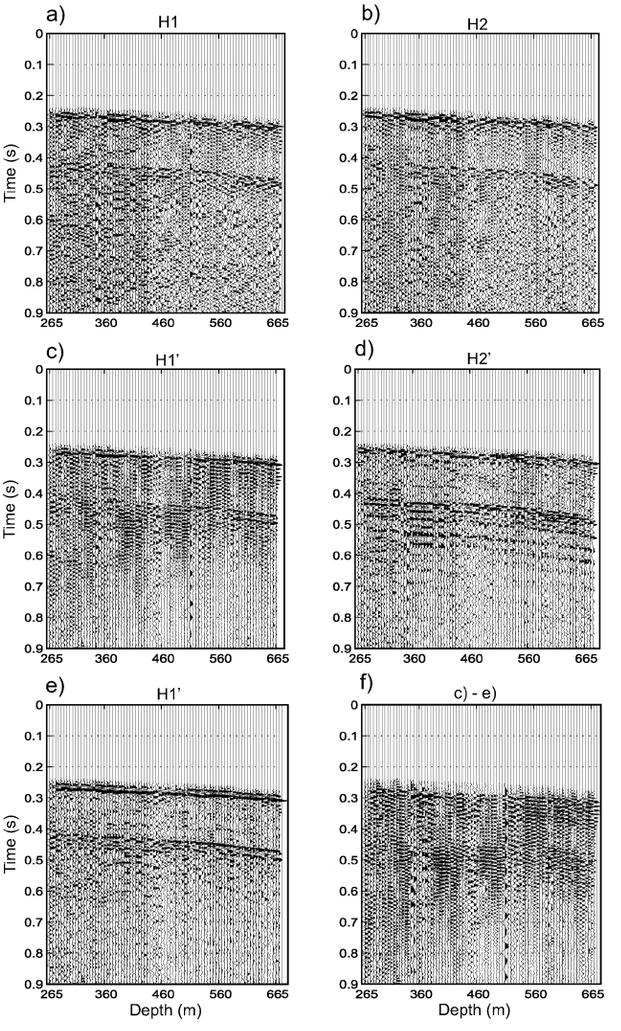

Figure 7. (a, b) Field records for two horizontal components from VSP site B. Some traces are characterized by a long oscillating coda after first arrivals. (c) Horizontal component 1 with maximized oscillating coda. (d) Horizontal component 2 after maximization. The H2 component does not contain the oscillations. (e) Results from predictive deconvolution on (c), showing that the oscillating coda was efficiently removed from the data. (f) Difference between (c) and (e). Data (d and e) were rotated back to their original position and transformed into radial and transverse orientations.

Offset VSP

Mode-converted waves are frequently observed and analyzed in offset VSP data acquired in sedimentary basins (Lash, 1982; Amhed, 1989; Geis et al., 1990) but are seldom observed or reported on VSP data recorded over or near known sulfide deposits in crystalline rocks. Elastic-wave theory and finite-difference modeling predict strong amplitudes for converted waves originating from a massive sulfide orebody (Bohlen et al., 2003). A VSP survey intersecting the Bell Allard massive sulfide deposit (Matagami, Québec) recorded P-waves and converted S-waves scattered at the orebody (Adam et al., 2003).

The downhole seismic data from Halfmile Lake show prominent scattered and converted P- and S-waves on all three components (see P-P, P-S, S-S, and S-P events on Figures 8 and 9). Such complex scattering from massive sulfide ore has not been observed previously in VSP data. Most of the scattered and converted waves originate from the deep sulfide lens intersected at the bottom of the borehole. This interpretation is based on calculations of the traveltime response for the deep lens for shot site B (Figure 8). Traveltimes were calculated for scatterers on the deep sulfide lens using a simple geometric ray modeling approach that assumes a scattering object can be represented by point scatterers on its surface. This approach accurately calculates traveltimes but does not account for the dynamics of the scattered amplitudes. We simulated a homogeneous background with P- and S-wave velocities of 5400 and 3050 m/s, respectively. These velocities were determined from direct P- and S-wave traveltimes. The purpose of this simplistic modeling approach was to support the identification of the various wave types and to demonstrate that a constant velocity medium provides a reasonable approximation for migration.

Scattered P-waves observed on the vertical component from all shot sites (Figures 8 and 9) are particularly continuous on sections from VSP sites A and B. Radial and transverse components are generally characterized by scattered S-waves and P-S and S-P converted waves, but all three wave modes are only observed simultaneously on the radial component from site B. The radial component from site C shows only strong P-S waves, whereas S-P waves predominate on the radial and transverse components from site D (Figure 9).

Finite-difference modeling and elastic-wave modeling of orebodies of various shapes and compositions demonstrates that scattering directivity is essentially controlled by the shape of the deposit (Eaton, 1999; Bohlen et al., 2003). At Halfmile Lake, this shape factor probably influenced the scattering response observed for each VSP. The north–northwest-dipping sulfide sheet offers a larger scattering surface for downgoing waves traveling from shot sites A and B and should focus

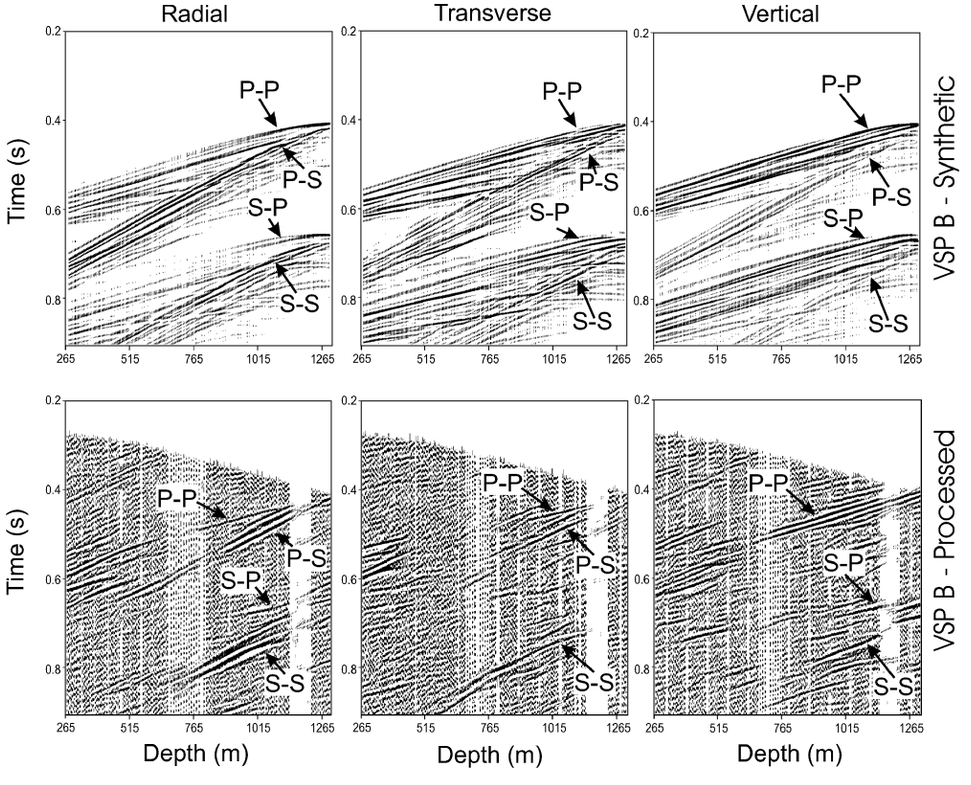

Figure 8. Synthetic and processed radial, transverse, and vertical components from shot site B. Synthetic data show the traveltime response for the deep sulfide lens only. The modeling approach accurately calculates traveltimes but does not account for the dynamics of the scattered amplitudes. Traveltimes indicate that most of the events on the processed data originate from the deep lens. Traveltimes were calculated with homogeneous background P- and S-wave velocities of 5400 and 3050 m/s, respectively. Polarizations were obtained by projecting the rays originating from scatterers located on the deep lens on the receiver components. Various events are annotated: P-P (incident P-wave, scattered P-wave), P-S (incident P-wave, scattered mode-converted S-wave), S-P (incident S-wave, scattered mode-converted P-wave), and S-S (incident S-wave, scattered S-wave).

backscattered energy in the direction of specular reflection from a planar interface with the same orientation and dip (Eaton, 1999). The acquisition borehole, located downdip of the HN99-119 discovery borehole, is well positioned to record the four scattered wave modes produced by incident waves from sites A and B. Direct waves traveling from sites C and D arrive at the sulfide sheets with a large incident angle, producing a scattered wavefield which may not have its strongest amplitude in the downdip direction, toward the recording borehole. Thus, the location of shot sites C and D, the shape of the deposit, and the position of the borehole likely explain why fewer wave modes were observed on records from these sites.

Another factor to consider when analyzing the scattering response at Halfmile Lake is the type and strength of downgoing waves generated at the source. The S-wave scattering or S-P converted waves can be expected only if a downgoing S-wave reaches the orebody. For example, VSP C shows weak downgoing S-waves, which were likely insufficient to produce strong S-S or S-P orebody scattering (see Figures 6 and 9). Downgoing S-waves are generated near the source or result from wave conversion at the surface or at the interface between the weathered and consolidated layers (Edelmann, 1985). Depending on near-surface conditions, both S_v- and S_h-waves can be generated. S_v-waves result from wave conversion at the surface or at the interface between the weathered and consolidated layers. S_h-waves can be generated by explosives detonated at strongly reflecting interfaces or in fractured media (Geyer and Martner, 1969). Although both downgoing S_v- and S_h-waves were recorded at Halfmile Lake (Figure 6), the strength of these S-waves varies from site to site because of varying near-surface conditions around the shot holes. The shots were fired in an overburden of variable thickness or in

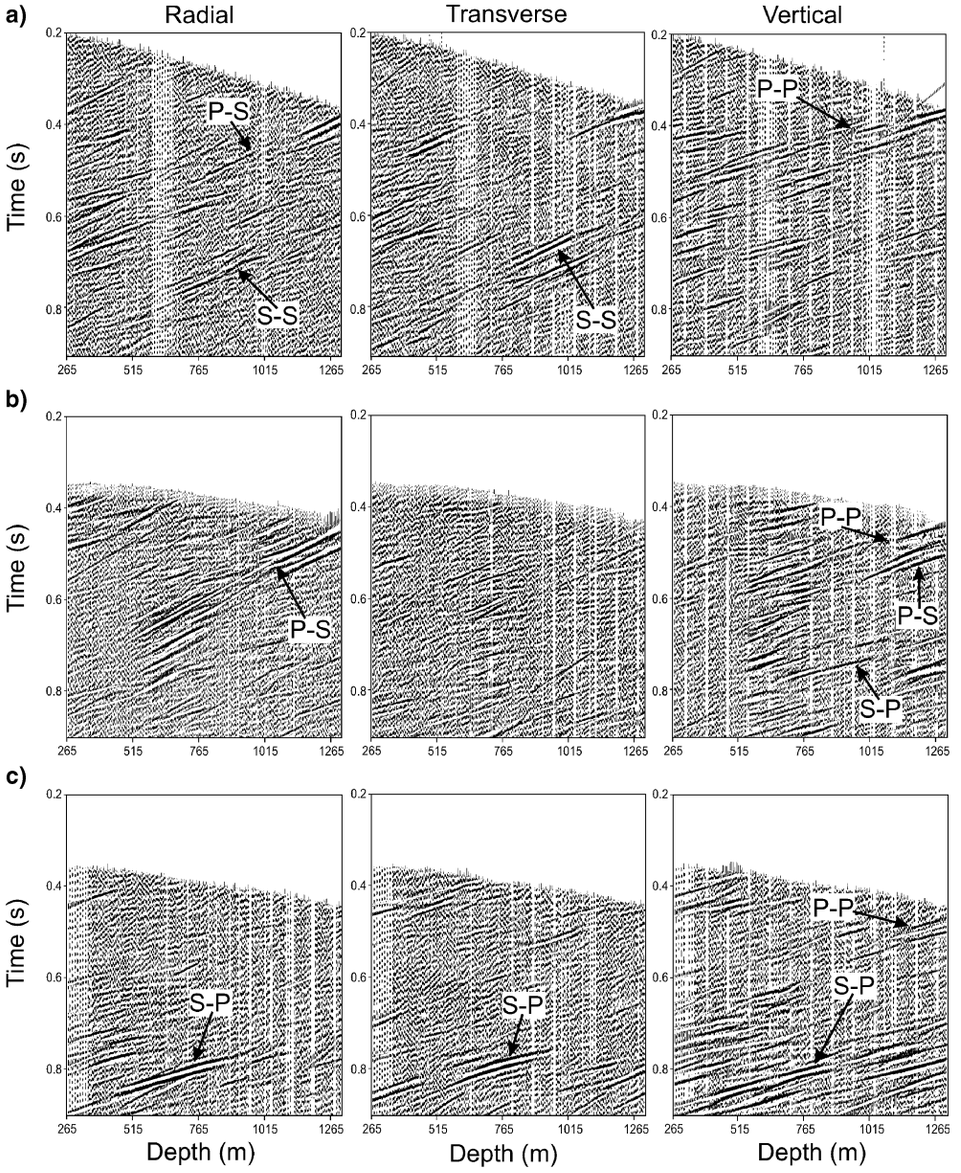

Figure 9. Radial, transverse, and vertical components from shot sites (a) A, (b) C, and (c) D after processing. The amplitude characteristics and occurrences of the scattered and converted events varies for each shot location.

highly fractured outcrops. These shots produced downgoing S-waves with slightly different characteristics for each site, which influenced the scattered wavefields.

Walkaway VSP

Figure 10 shows raw and processed vertical component data for selected shot points located on the shot line (see Figure 5 for shot location). The field records are dominated by downgoing P- and S-waves, in which the strength of the S-waves varies with shot site. A few field gathers show clear reflections close in arrival time to the direct S-waves. These reflections and others were enhanced by processing (Figure 10b). The mode determination of each event, based on its velocity, is complicated by the limited number of receiver positions used during acquisition. The radial and transverse components contain limited scattered events compared to the vertical component and could not be used to help determine mode. The scattered and mode-converted waves recognized on the vertical component data from VSP sites A, C, and D were used to help identify scattered waves from the walkaway survey (Figure 10b). Only scattered P-P-waves were consistently recognized.

MIGRATION OF THE SCATTERED WAVEFIELD

Polarization stack migration (Takahashi, 1995; Duveneck et al., 2004) was applied to the VSP data sets to determine the spatial origin of the scattered wavefield. This approach takes advantage of the three-component information to overcome the complexity of the scattered elastic wavefield and to reduce the spatial ambiguity inherent to the limited number of shotpoints used in the survey. However, polarization stack migration failed to image the sulfide lenses or any geological features in the Halfmile Lake area. A polarization analysis of the scattered events observed on the processed VSP data sets did not reveal linearly polarized waves or trends in polarization direction, except for the P-P scattered waves from VSP B. We suspect that useful polarization information was partly overprinted by the long oscillating coda observed after the direct P- and S-waves and/or modified by the predictive deconvolution operator applied to remove the coda. Potential errors in receiver positioning and orientation may also have degraded polarization information. As an alternative to vector migration, we selected a conventional traveltime migration algorithm.

A one-step migration combining all modes is complex because P- and S-wave velocities are required for the four wave propagation modes observed in the data. Dillon et al. (1988) suggest separating the waves according to their propagation mode prior to migration. Each mode is then migrated separately. Wavefield separation can be efficient for plane waves but is more difficult to accomplish for scattered waves originating from a relatively small orebody with complex shape. Such an orebody can also produce multiple interfering scattered and converted waves, which are even more difficult to

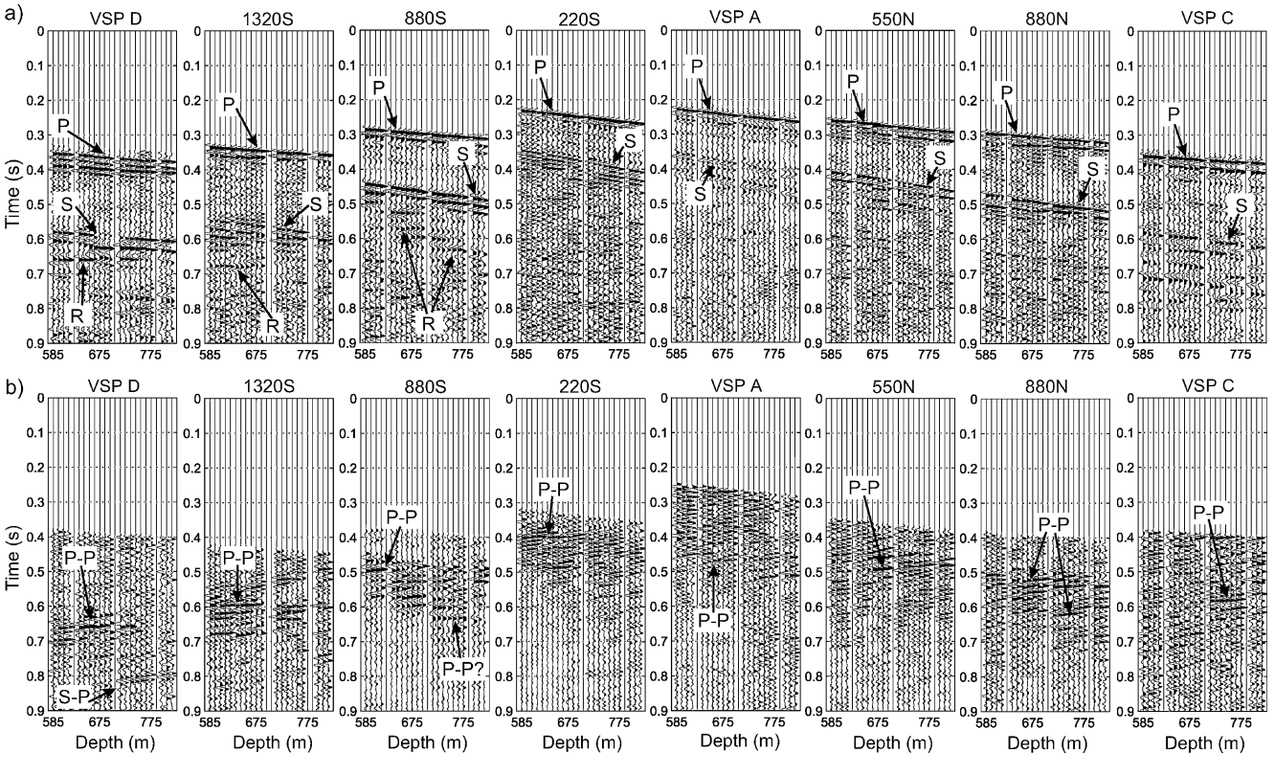

Figure 10. (a) Raw and (b) processed vertical component from several shot locations of the walkaway survey. Various events are annotated: P (direct P-wave), S (direct S-wave), R (reflection), P-P (scattered P-wave), P-S (scattered mode-converted S-wave), S-P (scattered mode-converted P-wave), and S-S (scattered S-wave). Raw data are shown with automatic gain control (AGC); processed data are shown with energy balancing. Portions of data from VSPs A, C, and D are shown to support identification of seismic events.

separate. Traces acquired close to the borehole-deposit intersection show some wave-mode interference (Figure 9).

Instead of attempting wavefield separation, we migrated data using a combination of velocities suitable for each converted mode. For example, P-S converted waves were migrated using P-wave velocity for source–subsurface point traveltimes and S-wave velocity for subsurface point–receiver traveltimes. A 3D prestack diffraction stack migration algorithm was used with homogeneous background P- and S-wave velocities of 5400 and 3050 m/s, respectively. The use of a constant-velocity model was motivated by borehole logging results. Each VSP component was migrated separately. A complication with this approach is that other modes present in the data and migrated with the wrong velocities will distort the image of the orebody in the migrated volume. Distortion is expected to be limited for data characterized mostly by one wave mode (e.g., radial and transverse components for VSP sites C and D, vertical component from the walkaway VSP). Because P- and S-wave velocities differ considerably, the distortion observed on other VSP data will unlikely appear close to the sulfide lenses (see, for example, S-S waves migrated with P-wave velocity on Figure 11). For scattered waves produced from the same incident wave mode (e.g., P-P and P-S, or S-S and S-P), the traveltime difference is relatively small at receiver positions close to the borehole-deposit intersection. Thus, amplitudes from the mode migrated with inappropriate combination of velocities are spread above or below the true sulfide lens position, whereas amplitudes from the correctly migrated mode should coincide with the deposit.

The migration results for four different wave modes observed on the offset VSP data are shown in Figure 11. The upper surface of the deep lens, as defined by drilling and an earlier surface 3D seismic survey, is also displayed on this Figure. Strong migrated energy from all four assumed wave-propagation modes coincides with the deep sulfide lens, although different portions of this lens are imaged with each mode. The migrated image of the P-P scattered waves recorded on the vertical component from the walkaway VSP also shows strong migrated energy at the deep lens (Figure 12). The consistent migrated images from both survey geometries indicate

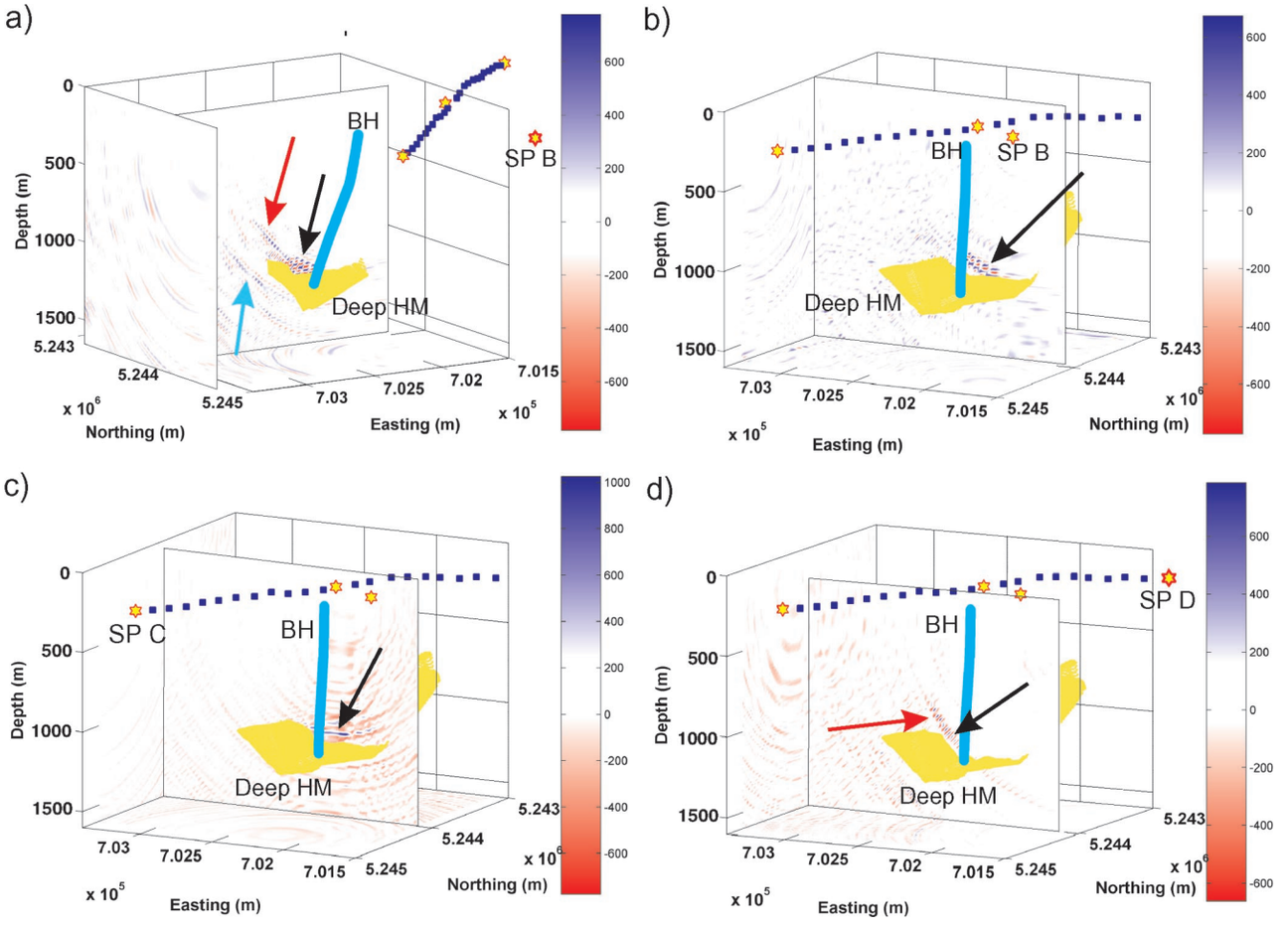

Figure 11. Migration of the four modes observed on the VSP data. Shotpoints (SP), borehole (BH), and the upper surface of the deep Halfmile lens (yellow surface) defined by drilling and 3D seismic data are displayed. Strongest energy (black arrows) for all four scattering modes coincides with the deep lens. Red arrows point to amplitudes migrated in the updip continuation of the deep lens, toward the area of steeply dipping stratigraphy. The blue arrow points to S-S scattered waves migrated with P-wave velocity. The 3D volume consists of 90 cells in the x- and y-directions and 80 cells in the vertical direction. Gridpoints were distributed every 20 m in the 3D volume. The color scale enhances maximum and minimum amplitudes.

that most of the strong scattered waves observed in the data originated from the deep lens. The lower lens and the area of steeply dipping stratigraphy between the two lenses are, at best, poorly imaged on the migrated sections. The migrated vertical component from VSP B and the radial component from VSP C show a reflector in the updip continuation of the deep lens, toward the area of steeply dipping stratigraphy (red arrows on Figure 11). These amplitudes are more likely migration artifacts.

Each VSP data set images a slightly different part of the deep sulfide lens. We have tentatively stacked all migrated volumes (4 VSP $\times$ 4 wave modes = 16migrated volumes) to define which part of the lens was effectively imaged and to reduce spatial ambiguity, typically observed as isochrone noise on individual migrated cubes. To minimize potential destructive interference from different frequency content of the P- and S-wave modes, absolute amplitude values were stacked. An isosurface display (equal amplitude values are connected by a surface) was chosen with a threshold value set to half of the maximum amplitude. The isosurfaces are spread over the northeast portion of the deep lens and in the target zone, as shown in Figure 13. The fit of isosurfaces with the deep lens is not perfect. Large-scale variations of the medium velocities and source statics partly explain the misfit. Wave modes migrated with inadequate combinations of velocities also disperse the isosurfaces above and below the true sulfide lens position.

DISCUSSION

The 3D seismic survey at Halfmile Lake provided the necessary information to accurately map the geometry of the acoustic impedance anomaly and also provided additional detail on size and thickness to help assess economic importance early in the drilling program (Gingerich et al., 2002; Matthews, 2002). The limited 3D coverage provided by the multioffset VSPs is not sufficient to map precisely the outline of the orebody or to provide thickness estimates. However, downhole seismic measurements, relatively inexpensive when compare to a 3D survey, provide a promising approach to locate and define a drill target. Furthermore, the strong amplitudes of the converted waves which were not observed or recognized on 3D seismic data provide additional imaging capabilities. They also indicate that great care must be taken when interpreting 3D data because converted waves, if processed as P-P waves, could generate coherent noise and artifacts on migrated data. To date, converted waves have been rarely considered during processing and interpretation of 3D seismic data acquired for mineral exploration purposes, yet they provide valuable additional information when processed correctly.

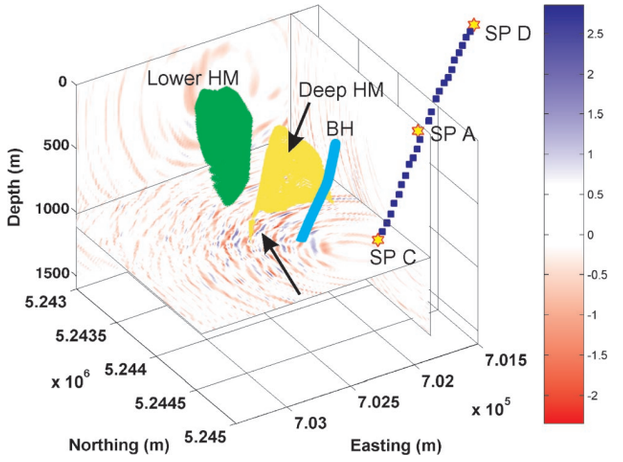

Figure 12. Migration of the vertical components from the walkaway VSP survey. The horizontal slice in the migrated data is located at a depth of 1100 m. Shotpoints (SP), borehole (BH), and the upper surface of the deep lens (yellow surface) defined by drilling and surface 3D seismic data are displayed. Large amplitudes (black arrow) coincides with the deep lens. Variations in source statics and localized velocity perturbations in the host rocks are possible explanations for the noisy image.

CONCLUSIONS

The Halfmile Lake deposit includes reflective massive sulfide lenses of known geometry, embedded in a low-reflectivity, steeply dipping hosting stratigraphy. The physical rock and sulfide properties in this environment are favorable for producing prominent scattered and mode-converted waves (P-P, P-S, S-S, and S-P) in downhole seismic data. In this data set, most prominent amplitudes are scattered energy originating from the deep lens of the deposit. The scattered wavefield recorded at Halfmile Lake is controlled by the shape of the orebody, the contrast in physical properties between sulfide lenses and host rocks, the acquisition geometry, and the downgoing wavefield generated at the source or modified by near-surface conditions. Although we are unable to image the shape of the lens exactly, migration of several wave modes observed on the VSP data could indicate the position of a strong reflector representing the deep sulfide lens. The scattered S-waves and mode-converted

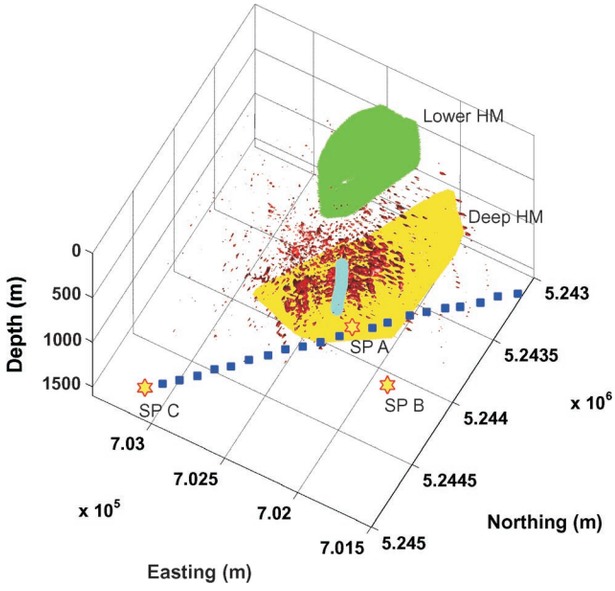

Figure 13. Stack of absolute amplitudes from all migrated volumes (4 VSP $\times$ 4 wave modes = 16 migrated volumes) displayed with isoamplitude surfaces. Amplitudes equal to half of the maximum amplitude are connected by a surface. The isosurfaces (in red) are spread over the northeast portion of the sulfide lens and in the area of steeply dipping stratigraphy connecting the lower and deep sulfide lenses. Isosurfaces located close to the deep lens–borehole intersection were defined primarily by the deep traces.

waves provide additional imaging capabilities which should be considered when applying downhole seismic methods to mining exploration.

ACKNOWLEDGMENTS

We thank Larry Petrie and Robert Banville for logistical support provided during field work and Noranda for permission to release these results. Erick Adam, Dave Forsyth, and Brian Roberts are thanked for field support at various stages of the project and for comments on an earlier version of this paper. Reviews by Bob Hardage and an anonymous reviewer substantially improved the quality of the final manuscript. Geological Survey of Canada contribution 2002044.

REFERENCES

Adair, R. N., 1992, Stratigraphy, structure, and geochemistry of the Halfmile Lake massive-sulfide deposit, New Brunswick: Exploration and Mining Geology, **1**, 151–166.

Adam, E., Bohlen, T., and Milkereit, B., 2003, Vertical seismic profiling at the Bell Allard orebody, Matagami, Quebec, *in* Milkereit, B., Eaton, D., and Salisbury, M., Eds., Hardrock seismic exploration: Society of Exploration Geophysicists, 181–193.

Adam, E., Perron, G., Milkereit, B., Wu, J., Calvert, A. J., Salisbury, M., Verpaelst, P., and Dion, D.-J., 2000, A review of high-resolution seismic profiling across the Sudbury, Selbaie, Noranda, and Matagami mining camps: Canadian Journal of Earth Sciences, **37**, 503–516.

Amhed, H., 1989, Application of mode-converted shear waves to rock-property estimation from vertical seismic profiling data: Geophysics, **54**, 449–457.

Bellefleur, G., Müller, C., Perron, G., and Snyder, D., 2001, Reliability of VSP–receiver orientations deduced from direct P-wave polarization: 71st Annual International Meeting, Society of Exploration Geophysicists, Expanded Abstracts, BH42.

Bellefleur, G., Müller, C., Snyder, D., Matthews, L., Forsyth, D., Roberts, B., and Tammadge, D., 2002, A new approach to downhole seismic imaging, Halfmile Lake, New Brunswick: Geological Survey of Canada Current Research 2002-D4.

Bohlen, T., Müller, C., and Milkereit, B., 2003, Elastic wave scattering from massive sulfide orebodies: On the role of composition and shape, *in* Milkereit, B., Eaton, D., and Salisbury, M., Eds., Hardrock seismic exploration: Society of Exploration Geophysicists, 70–83.

Dillon, P. B., Ahmed, H., and Roberts, T., 1988, Migration of mixed-mode VSP wavefield: Geophysical Prospecting, **36**, 825–846.

DiSiena, J. P., Gaiser, J. E., and Corrigan, D., 1984, Horizontal components and shear-wave analysis of three-component VSP data, *in* Toksoz, M. N., and Stewart, R. R., Eds., Vertical seismic profiling, part B: Advanced concepts: Geophysical Press, 177–189.

Duveneck, E., Müller, C., and Bohlen, T., 2004, Imaging of orebodies with vertical seismic profiling data, *in* Challenges for earth sciences in the 21st century: Springer, in press.

Eaton, D. W., 1999, Weak elastic wave scattering from massive sulfide orebodies: Geophysics, **64**, 289–299.

Eaton, D. W., Guest, S., Milkereit, B., Bleeker, W., Crick, D., Schmitt, D., and Salisbury, M., 1996, Seismic imaging of massive sulfide deposits: Part III, borehole seismic imaging of near-vertical structures: Economic Geology, **91**, 835–840.

Eaton, D. W., Milkereit, B., and Salisbury, M., 2003, Seismic methods for deep mineral exploration: Mature technologies adapted to new targets: The Leading Edge, **22**, 580–585.

Edelmann, H. A. K., 1985, Shear-wave energy source, *in* Dohr, G., Ed., Seismic shear waves, part B: Applications: Geophysical Press, 134–177.

Geis, W. T., Stewart, R. R., Jones, M. J., and Katopodis, P. E., 1990, Processing, correlating, and interpreting converted shear waves from borehole data in southern Alberta: Geophysics, **55**, 660–669.

Geyer, R. L., and Martner, S. T., 1969, SH waves from explosive sources: Geophysics, **34**, 893–905.

Gingerich, J. C., Peshko, M. J., and Matthews, L., 2002, The development of new exploration technologies at Noranda: Seeing more with hyperspectral and deeper with 3-D seismic: Canadian Institute of Mining Bulletin, **95**, 56–61.

Hardage, B. A., 2000, Vertical seismic profiling principles, *in* Helbig, K., and Treitel, S., Eds., Handbook of geophysical exploration: Pergamon Press.

Kong, S. M., Phinney, R. A., and Roy-Chowdhury, K., 1985, A nonlinear signal detector for enhancement of noisy seismic record section: Geophysics, **50**, 539–550.

Lash, C. C., 1982, Investigation of multiple reflections and wave conversion by means of a vertical wave test (vertical seismic profiling) in southern Mississippi: Geophysics, **47**, 977–1000.

Matthews, L., 2002, Base metal exploration: Looking deeper and adding value with seismic data: Recorder, **27**, 37–43.

McCutcheon, S. R., 1992, Base-metal deposits of the Bathurst-Newcastle district: Characteristics and depositional models: Exploration and Mining Geology, **1**, 105–119.

Milkereit, B., Berrer, E. K., King, A. R., Watts, A. H., Roberts, B., Adam, E., Eaton, D. W., Wu, J., and Matthews, L., 2000, Development of 3-D seismic exploration technology for deep nickel–copper deposits—A case history from the Sudbury basin, Canada: Geophysics, **65**, 1890–1899.

Salisbury, M., Milkereit, B., Ascough, G., Adair, R., Matthews, L., Schmitt, D. R., Mwenifumbo, J., Eaton, D. W., and Wu, J., 2000, Physical properties and seismic imaging of massive sulfides: Geophysics, **65**, 1882–1889.

Takahashi, T., 1995, Prestack migration using arrival angle information: Geophysics, **60**, 154–163.

Thomas, M. D., Walker, J. A., Keating, P., Shives, R., Kiss, F., and Goodfellow, W. D., 2000, Geophysical atlas of massive sulphide signatures, Bathurst mining camp, New Brunswick: Geological Survey of Canada Open File 3887.